Observation of the Keyhole during Plasma Arc Welding

Once the keyhole was established, the width of the keyhole did not change with an increasing welding current and a decreasing welding speed

BY Y. M. ZHANG AND S. B. ZHANG

ABSTRACT. Keyhole plasma arc welding is a unique arc welding process for deep penetration. To ensure the quality of the welds, the presence of the keyhole is critical. Understanding of the keyhole will certainly benefit the improvement of the process and weld quality. Currently, the size of the keyhole is assumed to be correlative with the robustness of the keyhole process in maintaining the keyhole. To verify this assumption, the keyhole and the weld pool were simultaneously monitored from the back side of the workpiece. It was found that once the keyhole is established, the width of the keyhole does not change with an increasing welding current and a decreasing welding speed. This implies the width of the keyhole gives no adequate information about the stable state of the keyhole and should not be used as an indication of the robustness of the keyhole process in plasma arc welding.

Introduction

Keyhole plasma arc welding (PAW) (Ref. 1) offers significant advantages over conventional gas tungsten arc welding (GTAW) in terms of penetration depth, joint preparation and thermal distortion (Ref. 2). Although its energy is less dense than laser beam welding (LBW) (Ref. 3) and electron beam welding (EBW) (Ref. 3), keyhole PAW is more cost effective and more tolerant of joint preparation (Ref. 4). Because of these distinct attributes, keyhole PAW has found applications on the welding of structural steels (Ref. 5), automobiles (Ref. 6), airplanes (Ref. 7), rockets (Ref. 8), space shuttles (Ref. 9) and possibly on welding in space (Ref. 10).

Although keyhole PAW had potential to replace GTAW (Ref. 1) in many applications as a primary process for precise joining, its complexity and equipment cost slowed this expansion initially (Ref. 1). During the late 1970s, remarkable achievements were made in simplifying the plasma cutting process, which originally was just as complex to use as PAW (Ref. 1). As a result, the complexity and equipment cost of PAW were significantly reduced. Now, cost and complexity are no longer the major factors preventing the expansion of PAW to further industrial applications.

The stable state of the keyhole is an important issue in applying PAW (Ref. 5). Although the stability of the keyhole has been a concern in many research works (Refs. 5, 11–16), no accurate definition has been given. Concerning weld quality control, the minimum requirement is the maintenance of the existence of the keyhole. It seems that precise control of keyhole size could be an effective approach to achieving a stable keyhole process and quality welds. Thus, studies have been conducted to correlate the keyhole size to the welding parameters that determine weld quality (Refs. 10, 11, 16, 17).

In a paper by Tomsic and Jackson (Ref. 11), the plasma arc was terminated during welding. The workpiece was then sectioned to measure the keyhole. The results were both the back-side width and the weld-face width of the keyhole increased as the current increased or the welding speed decreased (Ref. 11). This suggested the widths of the keyhole as indicators of the stable state of the keyhole PAW process. Metcalfe and Quigley mounted a photo-transistor at the end of the workpiece to monitor the efflux plasma from the underside (Ref. 16). The welding current was changed to establish different modes associated with plasma arc welding: stable keyhole, unstable keyhole and nonkeyhole. They found that the photoelectric measurement of the light emitted from the underside of the keyhole offered a basis for monitoring the keyhole PAW process (Ref. 16). In more recent efforts, keyhole PAW processes were numerically simulated (Refs. 4, 10, 17–20). However, only Keanini and Rubinsky extensively studied the correlation between the keyhole and the welding parameters during stationary welding (Ref. 10).

Due to a recent development in imaging technology (Ref. 21), the arc welding process can now be clearly observed despite the arc light. It is expected that clear observation of the keyhole and the weld pool will provide more reliable data for analyzing the correlation between the geometry of the keyhole and its stable state or the robustness of the process in maintaining the keyhole. The findings would be fundamental in guiding the development of sensing and control technologies for keyhole PAW, thus facilitating the applications of this unique process.

KEY WORDS

Bead-on-Plate Welds
Butt Joint Welds
Flow Rate
Keyhole
Stainless Steel
Orifice Diameter
Plasma Arc Welding

Experimentation

Experimental Setup

The experimental setup is shown in Fig. 1. The power supply is an inverter designed for gas tungsten arc welding and plasma arc welding. Its current ranges from 10 to 200 A and is precisely controlled by an inner-loop controller. The host computer adjusts the welding current through the analog output interface to the power supply. The torch, a regular commercial straight-polarity plasma arc welding torch rated at 200 A, and the camera are attached to a manipulator. The motion of the manipulator is computer controlled.

An ultra-high shutter speed vision sys-

Y. M. ZHANG and S. B. ZHANG are with the Welding Research and Development Laboratory, Center for Robotics and Manufacturing Systems, University of Kentucky, Lexington, Ky.

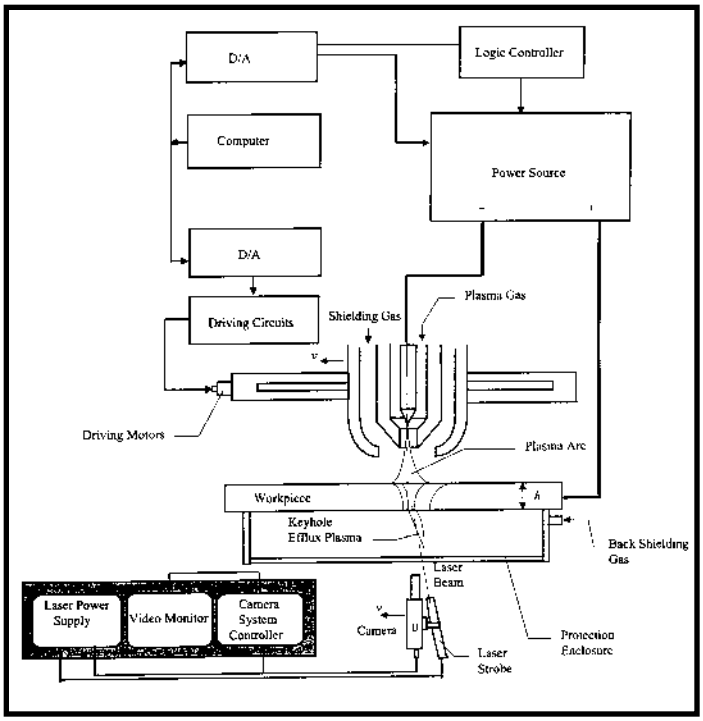

Fig. 1— Experimental Setup.

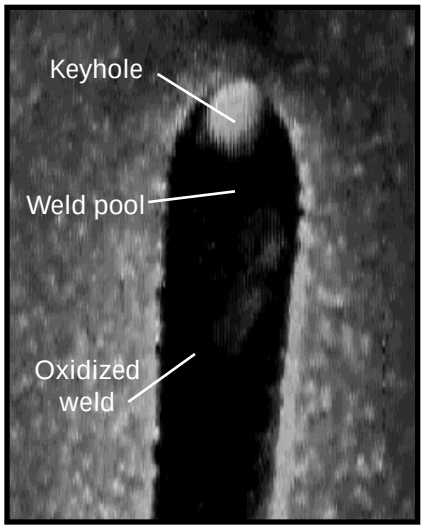

Fig. 2 — Simultaneous imaging of weld pool and keyhole.

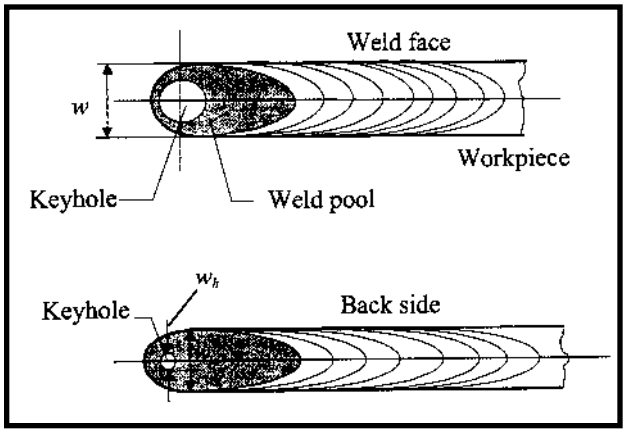

Fig. 3 — Geometrical parameters of weld pool and keyhole.

tem (Ref. 21) was used to simultaneously image the keyhole and the weld pool from the back side of the workpiece — Fig. 1. The camera system consisted of a strobe-illumination unit (pulse laser), camera head and system controller. The pulse duration of the laser was 3 ns, and the camera was synchronized with the laser pulse. Thus, the intensity of laser illumination during the peak was much higher than that of the plasma. Using this vision system, the weld pool would always be clearly observed and the plasma from the keyhole completely eliminated from the image (Ref. 22). In this study, both the keyhole and the weld pool need to be imaged. By increasing the illumination area of the laser, the brightness of the laser illumination could be reduced so that it was close to the brightness of the plasma. Both the keyhole and the weld pool could, therefore, be imaged clearly and simultaneously — Fig. 2. The weld-face width of the weld pool was measured off-line after the experiment using a structured-light 3-D vision sensor and a vision algorithm developed in previous work (Ref. 23).

Experimental Procedure

Bead-on-plate and butt-joint welds were made on 3-mm-thick stainless steel (304) plates in the flat position. Pure argon was used as the shielding gas and the plasma gas. The back side of the workpiece was also shielded using pure argon. The flow rate of the shielding gas was 16.5 L/min (35 ft³/h) and 9.4 L/min (20 ft³/h) for the weld face and the back side, respectively. The flow rate of the plasma gas, the welding current and the welding speed ranged from 1.3 L/min (2.8 ft³/h) to 2.6 L/min (5.5 ft³/h), from 55 to 95 A and from 1 to 3.5 mm/s.

Results and Discussion

Assume the keyhole has been established under certain welding parameters and conditions. If we decrease the welding current or increase the welding speed, the keyhole will eventually collapse. Or, if we increase the welding current or decrease the weld speed, burn-through (a hole in the root bead) may occur. Of course, the changes in other welding parameters or conditions may also cause the collapse and/or burn-through. The minimum changes in the welding parameters or conditions that result in either collapse or burn-through can quantify the capability or the robustness of the process in maintaining a stable keyhole or the stable state of the keyhole process. In the following discussion, the stable state of the keyhole process will be used as a term to describe the robustness of the process withstanding the perturbations in welding parameters and conditions for maintaining a stable keyhole.

The geometrical parameters defined in Fig. 3 will be used to illustrate the experimental results. They include the weld-face width of the weld pool (w), the back-side width of the weld pool (w_b) and the back-side width of the keyhole (w_h).

Welding Current and Speed

To verify the suggestion that the size of the keyhole is correlative with the stable state of the keyhole process, experiments were conducted using varying welding parameters. The method was to change the stable state of the keyhole and then examine whether there is a corresponding change in the keyhole size. The keyhole size was measured by using the back-side width of the keyhole as defined in Fig. 3. The welding speed and welding current were changed to alter the stable

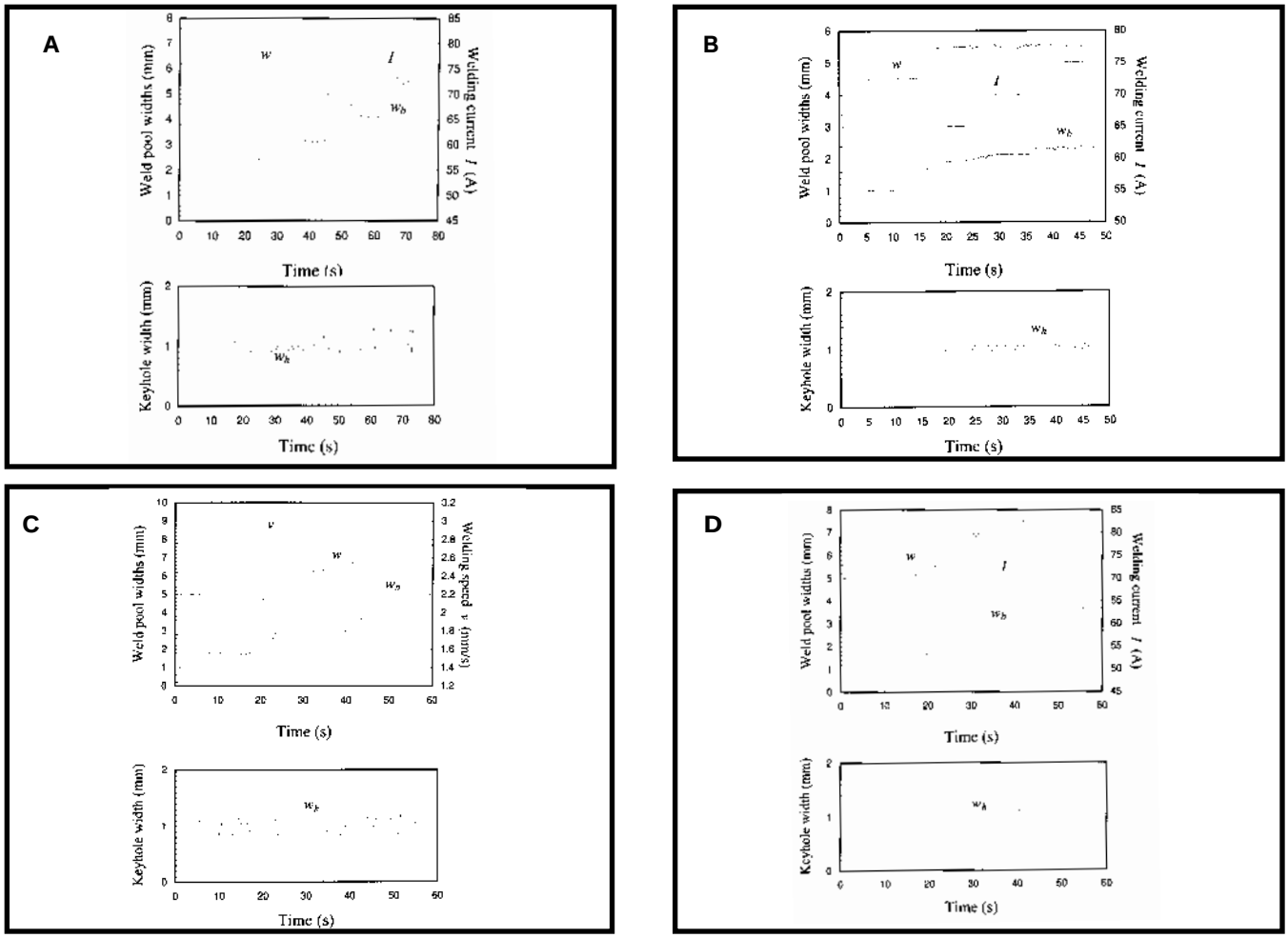

Fig. 4 — Weld pool and keyhole under varying welding parameters. Plasma gas flow: 1.3 L/min (2.8 ft³/h), orifice diameter: 1.57 mm (0.062 in.). A — Bead on plate, welding speed 2 mm/s; B — bead on plate, welding speed 2.8 mm/s; C— bead on plate, welding current 65 A; D — butt-joint weld, welding speed 2.2 mm/s.

state of the keyhole process.

Figure 4 shows the results of four experiments conducted using an increasing current or a decreasing speed. Both bead-on-plate and butt-joint welds were made. The flow rate of the plasma gas and the diameter of the orifice were the same for the four experiments. As shown in Fig. 4, when the welding current increased or the welding speed decreased to certain levels, the keyhole was established. Although the further increase in the welding current or the further decrease in the welding speed increased w and w_b, the width of the keyhole (w_h) did not change correspondingly: w_h remained at approximately 1 mm. The same phenomenon can be observed from the images given in Fig. 5.

The experimental results in Figs. 4 and 5 showed that the width of the keyhole was not changed by varying the welding current or the welding speed when no burn-through or collapse occurred. It would be interesting to examine whether the width of the keyhole will change if a burn-through or a collapse is about to occur.

In Fig. 6, the burn-through eventually takes place for all four experiments. The cause of the burn-through was the increase in the welding current or the decrease in the welding speed, and both bead-on-plate and butt joint weld experiments were conducted. Experimental results clearly demonstrated that the width of the keyhole did not provide any information or indication about the burn-through that was about to occur. Also, experiments have been performed using a decreasing welding current or an increasing welding speed to cause a collapse of the keyhole. An example is illustrated in Fig. 7. It can be seen that the width of the keyhole failed to predict the collapse.

When the welding current increases or the welding speed decreases, the stable state of the key-

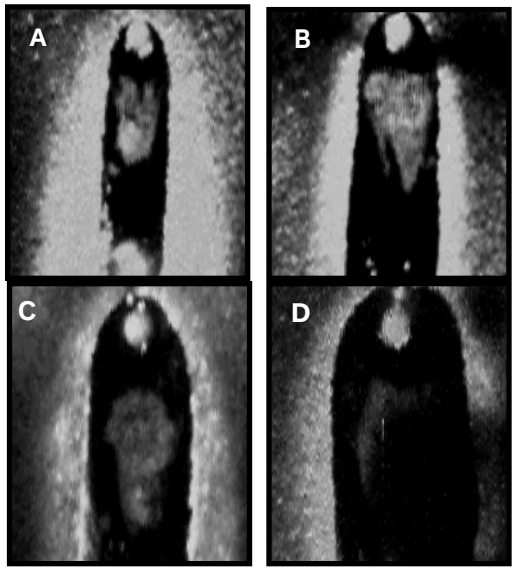

Fig. 5 — Back-side view of keyhole and weld pool at different currents and welding speeds. Plasma gas flow: 1.3 L/min (2.8 ft³/h), orifice diameter: 1.57 mm (0.062 in.). A — Welding speed 2 mm/s, welding current 60 A; B— welding speed 2 mm/s, welding current 65 A; C — welding speed 1.8 mm/s, welding current 70 A; D — welding speed 1.6 mm/s, welding current 75 A.

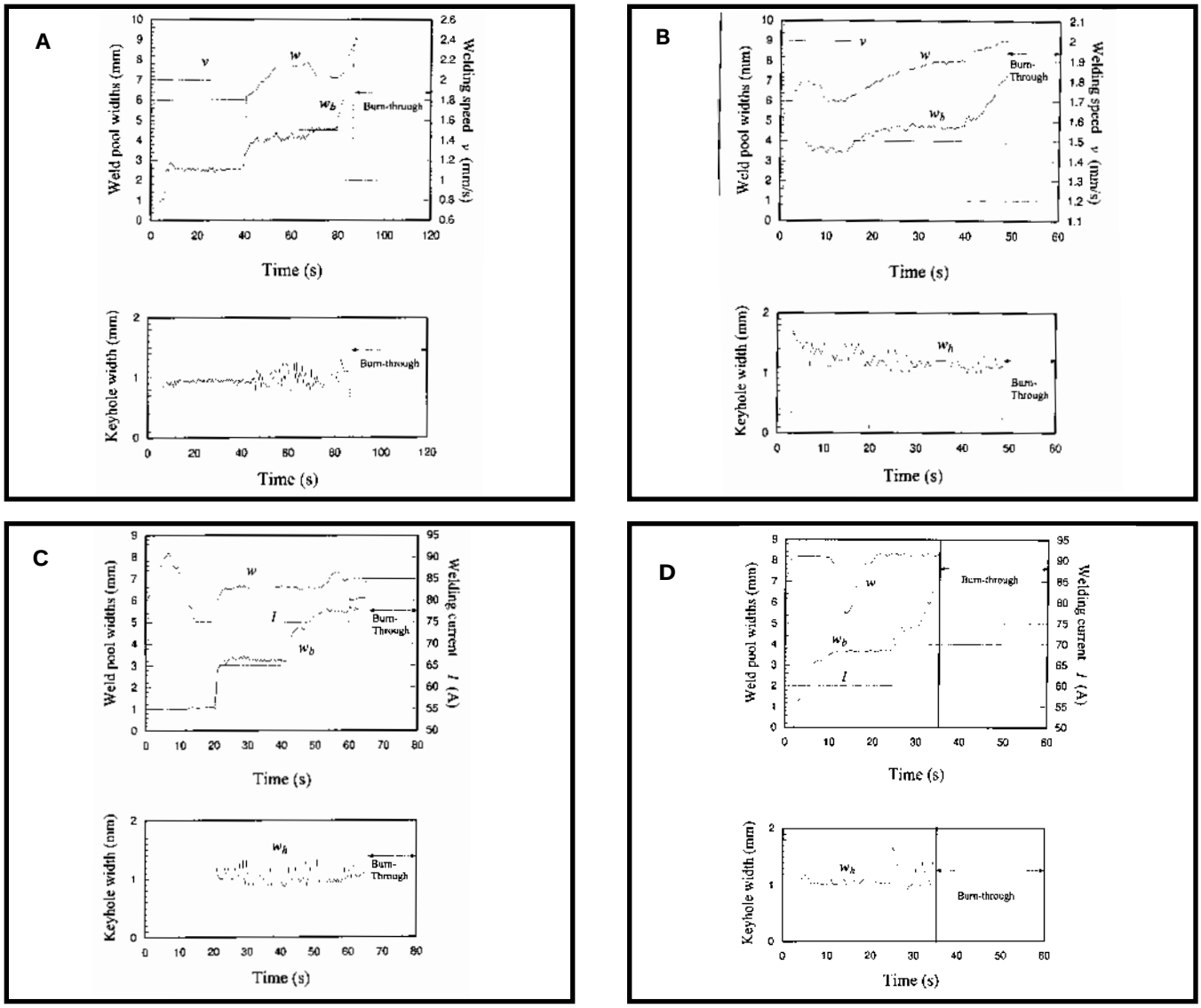

Fig. 6 — Burn-through experiments. Orifice diameter: 1.57 mm (0.062 in). A — Bead on plate, welding current 55 A, plasma gas flow 1.3 L/min (2.8 ft³/h); B — butt-joint weld, welding current 63 A, plasma gas-flow rate 1.6 L/min (3.4 ft³/h); C — bead on plate, welding speed 2 mm/s, plasma gas-flow rate 1.3 L/min (2.8 ft³/h); D— butt-joint weld, welding speed 1.6 mm/s, plasma gas-flow rate 1.3 L/min (2.8 ft³/h).

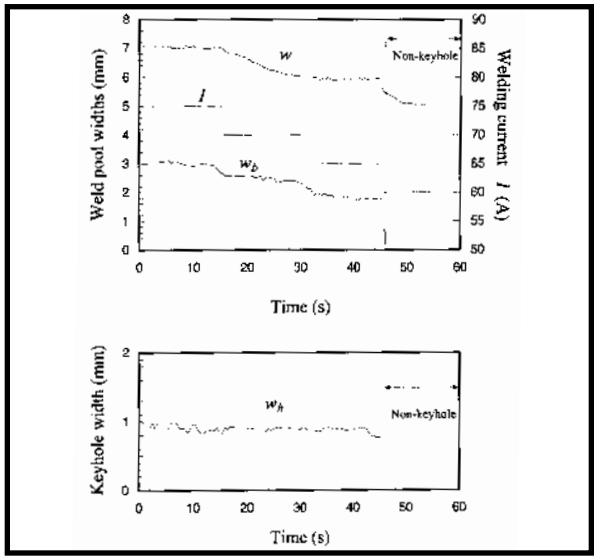

Fig. 7 — Keyhole collapse due to decrease in welding current. Butt-joint weld, welding speed: 2.4 mm/s, plasma gas-flow rate: 1.3 L/min (2.8 ft³/h), orifice diameter: 1.57 mm (0.062 in).

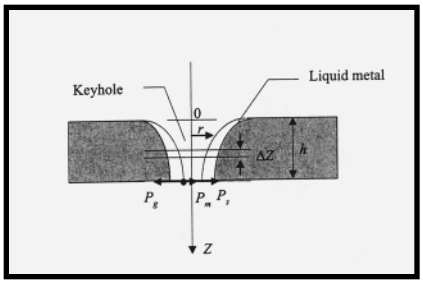

Fig. 8 — Horizontal forces acting on keyhole wall.

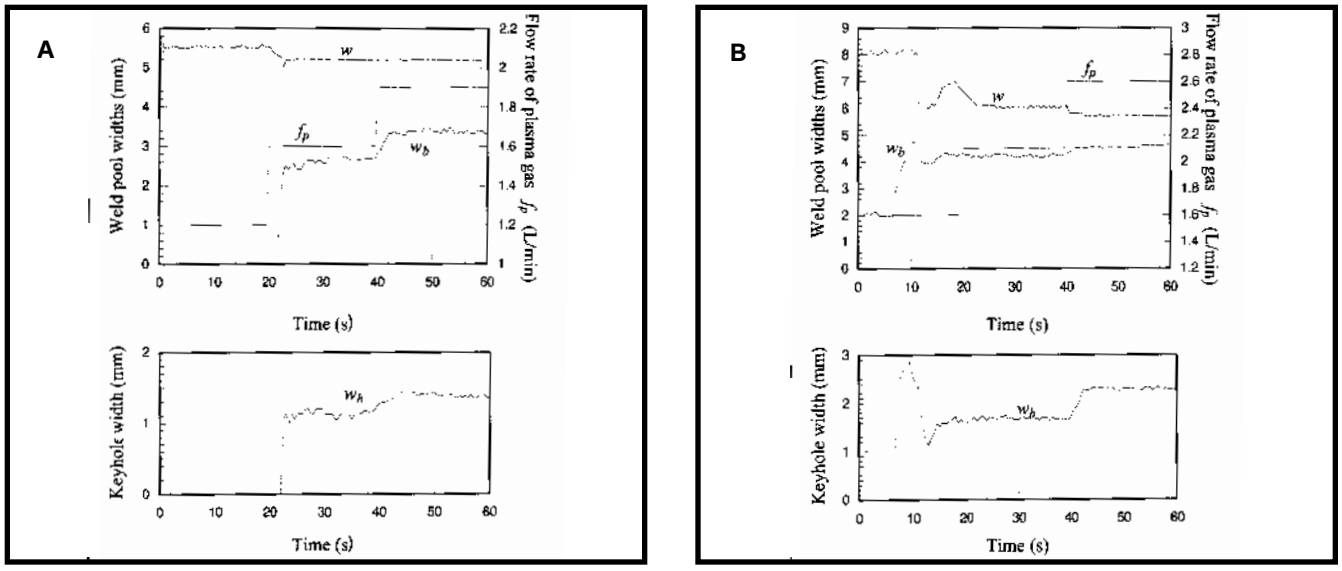

Fig. 9 — Plasma keyhole arc welding using varied rate of plasma gas flow (bead on plate). A — Welding speed 2.8 mm/s, welding current 65 A, orifice diameter 1.57 mm (0.062 in); B — welding speed 3 mm/s, welding current 95 A, orifice diameter 2.36 mm (0.093 in).

hole changes accordingly. For example, when the keyhole is barely established, a slight decrease in the welding current and/or the flow rate of the plasma gas or a slight increase in the welding speed may result in a collapse of the keyhole. This implies that the stable state of the keyhole needs to be improved to prevent the collapse. If the welding current and the flow rate of the plasma gas are increased and/or the welding speed is decreased, the process will withstand larger variations in the welding parameters, such as the welding current, the flow rate of the plasma gas and the welding speed, without a collapse of the keyhole. The stable state of the keyhole is improved. After the welding current and the flow rate of the plasma gas increase and/or the welding speed decreases to certain levels, further increase in the welding current and the flow rate of the plasma gas or decrease in the welding speed may cause a burn-through. The stable state degrades. Hence, when the welding current or the welding speed changes, the stable state of the keyhole process in terms of maintaining a stable keyhole changes accordingly.

Experimental results in Figs. 4, 6 and 7 demonstrated, when the stable state of the keyhole varied due to a change in the welding current or in the welding speed, the width of the keyhole remained constant. Therefore, the width of the keyhole is not correlative with the stable state of the keyhole process or the robustness of the process in maintaining a stable keyhole. Also, full penetration is measured using the back-side bead width of the weld pool (Refs. 24, 25). In the experiments, the back-side bead width w_b did change when the welding parameters were changed. Therefore, in addition to the stable state of the keyhole process, the width of the keyhole is also not correlative with the weld penetration.

Analysis

The independence of the width of the keyhole on the welding current and the welding speed is quite understandable. In fact, once the keyhole is established, the plasma gas passes through the keyhole. Because the majority of the welding current earths at the top surface of the weld pool (Ref. 26), the stagnation pressure of the plasma gas flow plays a major role in balancing with the surface tension pressure plus the hydrostatic head to keep the keyhole open (Refs. 10, 16).

The horizontal forces acting on the keyhole wall are shown in Fig. 8. The surface tension pressure that tends to close the keyhole is (Refs. 16, 27)

$$P_s = T_s / r \tag{1}$$

where T_s is the surface tension constant and r is the radius of the keyhole. (The keyhole is assumed to be axially symmetric.) The pressure generated by the hydrostatic head of the melted weld metal is (Ref. 16)

$$P_m = \rho_m g z \tag{2}$$

where ρ_m is the density of the liquid metal, g is the gravity acceleration and z is the coordinate along the thickness direction — Fig. 8. At the bottom surface of the plate, $r = w_h/2$ and $z=h$. Divide the keyhole as thin circular elements along the z direction. The thickness of a thin circular element is Δz. Assume that the mass of the plasma gas in any Δz, denoted by Δm, does not change with z. It is further assumed that $\Delta m/\Delta z$ is only determined by the flow rate of the plasma gas f_p and the speed of the plasma gas flow u. When f_p is given, u depends on the diameter of the orifice. From the ideal gas law (Ref. 28), the plasma gas stagnation pressure P_g can be expressed as

$$P_g = k' \frac{\Delta m(f_p, u)}{\pi r^2 \Delta z} = k \frac{\dot{m}(f_p, u)}{r^2} \tag{3}$$

where $\dot{m}$ is defined as $\Delta m/\Delta z$, and k' and K are coefficients. When the keyhole is stationary, the stagnation pressure of the plasma gas flow should balance the surface tension pressure and the pressure generated by the hydrostatic head. Equations 1–3 show that for the given material and plate thickness h, the back-side width of the keyhole is only controlled by T_s, f_p and u.

The surface tension constant T_s is temperature dependent. When the welding current or the welding speed changes, the temperature of the plasma, and, therefore, the temperature of the keyhole surface, should change. However, for a given material, one may assume that the temperature of the keyhole surface, especially at the bottom of the keyhole, is not subjected to a severe change. Hence, once the keyhole is established and the heat input is sufficient to melt enough material, changes in both the welding current and the welding speed should not

have a substantial influence on the back-side width of the keyhole.

That the width of the keyhole is not dependent on the welding current has also been indirectly obtained for stationary keyhole PAW by Keanini and Rubinsky (Ref. 11) based on numerical analysis. In their study, the heat input was measured by the initial plasma temperature rather than the welding current and the welding speed. It was found that the diameter of the keyhole, thus, the width, at any given axial position is independent of the initial plasma temperature (Ref. 11). Although the study did not attempt to correlate the initial plasma temperature with the electric power inputs, they claimed that plasma isotherms for various arc power inputs nevertheless confirmed that the initial plasma conditions are comparable to the initial plasma temperature. Keanini and Rubinsky's numerical analysis supports the fact that the back-side width of the keyhole is independent of the welding current during stationary keyhole PAW.

Flow Rate and Orifice

Although the back-side width of the keyhole is independent of the welding current and the welding speed, the flow rate of the plasma gas and the diameter of the orifice both have significant influences on the width of the keyhole. This can be seen from the dependence of the stagnation pressure of the plasma gas on the flow speed, which can be changed by altering the diameter of the orifice and the flow rate of the plasma gas. As can be observed from Fig. 9, for a given orifice, the back-side width of the keyhole increases as the flow rate of the plasma gas increases. Also, a larger width of the keyhole resulted in Fig. 9B due to the larger diameter of the orifice. It is known that the stable state of the keyhole changes with the flow rate of the plasma gas and the diameter of the orifice. Thus, in the case where a change in the stable state is caused by the plasma gas or the diameter of the orifice, the width of the keyhole gives information about the change in the stable state. However, the stable state of the keyhole process may be caused by different welding parameters, including the welding current and the welding speed. Therefore, in general, the width of the keyhole and the stable state of the keyhole process are not inherently correlated.

Summary

Bead-on-plate and butt-joint weld experiments have been conducted on 3-mm-thick stainless steel plates to verify the feasibility of using the back-side width of the keyhole as a measurement of the stable state of the keyhole process. Experimental results revealed that once the keyhole is established, the width of the keyhole does not change with the changes in the welding current and the welding speed, but it does change with the changes in the flow rate of the plasma gas and the diameter of the orifice. On the other hand, the stable state of the keyhole process and the weld-joint penetration vary when either the welding current, the welding speed or the flow rate of the plasma gas changes. Hence, the width of the keyhole gives no adequate information on the state of the keyhole process and the weld-joint penetration. Also, it provides no predictions of the burn-through and the collapse that are about to occur. Therefore, in general, the width of the keyhole should not be recommended as a critical parameter to monitor and control either the keyhole process or the weld-joint penetration.

References

1. Craig, E. 1988. The plasma arc welding — a review. *Welding Journal* 67(2): 19–25.
2. Tomsic, M., and Barhorst, S. 1984. Keyhole plasma arc welding of aluminum with variable polarity power. *Welding Journal* 63(2): 25–32.
3. *Welding Handbook, Vol. 2: Welding Processes.* 1991. 8th edition, American Welding Society, Miami, Fla.
4. Hsu, Y. F., and Rubinsky, B. 1988. Two-dimensional heat transfer study on the keyhole plasma arc welding process. *International Journal of Heat and Mass Transfer* 31(7): 1409–1421.
5. Martikainen, J. K., and Moisio, T. J. I. 1993. Investigation of the effect of welding parameters on weld quality of plasma arc keyhole welding of structural steels. *Welding Journal* 72(7): 329-s to 340-s.
6. Vilkas, E. P. 1991. Plasma arc welding of exhaust pipe system components. *Welding Journal* 70(4): 49–52.
7. Irving, B. 1997. Why aren't airplanes welded? *Welding Journal* 76(1): 31–41.
8. Irving, B. 1992. Plasma arc welding takes on the advanced solid rocket motor. *Welding Journal* 71(12): 49–50.
9. Nunes, A. C., *et al.* 1984. Variable polarity plasma arc welding on the space shuttle external tank. *Welding Journal* 63(9): 27–35.
10. Keanini, R. G., and Rubinsky, B. 1990. Plasma arc welding under normal and zero gravity. *Welding Journal* 69(6): 41–50.
11. Tomsic, M. J., and Jackson, C. E. 1974. Energy distribution in keyhole mode plasma arc welds. *Welding Journal* 53(3): 109-s to 115-s.
12. Bashenko, V. V., and Sosnin, N. A. 1988. Optimization of the plasma arc welding process. *Welding Journal* 67(10): 233-s to 237-s.
13. Martinez, L. F., *et al.* 1992. Front side keyhole detection in aluminum alloys. *Welding Journal* 71(5): 49–52.
14. Martikainen, J. 1995. Conditions for achieving high-quality welds in the plasma-arc keyhole welding of structural steels. *Journal of Materials Processing Technology* 52: 68–75.
15. Halmoy, E., Fostervoll, H., and Ramsland, A. R. 1994. New applications of plasma keyhole welding. *Welding in the World* 34: 285–291.
16. Metcalfe, J. C., and Quigley, M. B. C. 1975. Keyhole stability in plasma arc welding. *Welding Journal* 54(11): 401-s to 404-s.
17. Kim, C.-J. 1994. Parametric study of the two-dimensional keyhole model for high power density welding processes. *ASME Journal of Heat Transfer* 116(1): 209–214.
18. Dowden, J., and Kapadia, P. 1994. Plasma arc welding: a mathematical model of the arc. *Journal of Physics (D): Applied Physics* 27: 902–910.
19. Nehad, A.-K. 1995. Enthalpy technique for solution of stefan problems: application to the keyhole plasma arc welding process involving moving heat source. *International Communications in Heat and Mass Transfer* 22(6): 779–790.
20. Hung, R. J., and Long, Y. T. 1996. Mathematical model of variable polarity plasma arc welding process. *Proceedings of the National Science Council (A): Physical Science and Engineering* 20(1): 90–109.
21. Hoffman, T. 1991. Real-time imaging for process control. *Advanced Material & Processes* 140(3): 37–43.
22. Kovacevic, R., Zhang, Y. M., and L. Li. 1996. Monitoring of weld penetration based on weld pool geometrical appearance. *Welding Journal* 75(10): 317-s to 329-s.
23. Zhang, Y. M., and Kovacevic, R. 1997. Real-time sensing of sag geometry during GTA welding. *ASME Journal of Manufacturing Science and Engineering* 119(2): 151–160.
24. Zacksenhouse, M., and Hardt, D. E. 1983. Welding pool impedance identification for size measurement and control. *ASME Journal of Dynamic Systems, Measurement, and Control* 105(3): 179–184.
25. Zhang, Y. M., Wu, L., Walcott, B. L., and Chen, D. H. 1993. Determining joint penetration in GTAW with vision sensing of weld-face geometry. *Welding Journal* 72(10): 463-s to 469-s.
26. Dowden, J., Kapadia, P., and Fenn, B. 1993. Space charge in plasma arc welding and cutting. *Journal of Physics (D): Applied Physics* 26: 1215–1223.
27. Kroos, J., Gratzke, U., and Simon, G. 1993. Towards a self-consistent model of the keyhole in penetration laser beam welding. *Journal of Physics (D): Applied Physics* 26: 474–480.
28. Evett, J. B., and Liu, C. 1987. *Fundamentals of Fluid Mechanics*, McGraw-Hill Book Company, New York, N.Y.